Transparent Gold as a Platform for Adsorbed Protein Spectroelectrochemistry: Investigation of Cytochrome c and Azurin

ARTICLE *in* LANGMUIR · FEBRUARY 2012

Impact Factor: 4.46 · DOI: 10.1021/la300404r · Source: PubMed

6 AUTHORS, INCLUDING:

Olaf Schulz
Georg-August-Universität Göttingen
11 PUBLICATIONS **119** CITATIONS
SEE PROFILE

Chelsea Lee McIntosh
Washington University in St. Louis
7 PUBLICATIONS **73** CITATIONS
SEE PROFILE

Iddo Pinkas
Weizmann Institute of Science
34 PUBLICATIONS **652** CITATIONS
SEE PROFILE

Robert Ros
Arizona State University
89 PUBLICATIONS **1,980** CITATIONS
SEE PROFILE

Langmuir

Article

pubs.acs.org/Langmuir

Transparent Gold as a Platform for Adsorbed Protein Spectroelectrochemistry: Investigation of Cytochrome *c* and Azurin

Idan Ashur,[†] Olaf Schulz,[‡] Chelsea L. McIntosh,[†] Iddo Pinkas,[⊥] Robert Ros,[‡] and Anne K. Jones*[,†,§]

[†]Department of Chemistry and Biochemistry, [‡]Department of Physics, and [§]Center for Bioenergy and Photosynthesis, Arizona State University, Tempe, Arizona 85287, United States

[⊥]Department of Plant Sciences, The Weizmann Institute of Science, Rehovot, Israel

Supporting Information

ABSTRACT: The majority of protein spectroelectrochemical methods utilize a diffusing, chemical mediator to exchange electrons between the electrode and the protein. In such methods, electrochemical potential control is limited by mediator choice and its ability to interact with the protein of interest. We report an approach for unmediated, protein spectroelectrochemistry that overcomes this limitation by adsorbing protein directly to thiol self-assembled monolayer (SAM) modified, thin (10 nm), semitransparent gold. The viability of the method is demonstrated with two diverse and important redox proteins: cytochrome *c* and azurin. Fast, reversible electrochemical signals comparable to those previously reported for these proteins on ordinary disk gold electrodes were observed. Although the quantity of protein in a submonolayer adsorbed at an electrode is expected to be insufficient for detection of UV−vis absorption bands based on bulk extinction coefficients, excellent spectra were detected for each of the proteins in the adsorbed state. Furthermore, AFM imaging confirmed that only a single layer of protein was adsorbed to the electrode. We hypothesize that interaction of the relatively broad gold surface plasmon with the proteins' electronic transitions results in surface signal enhancement of the molecular transitions of between 8 and 112 times, allowing detection of the proteins at much lower than expected concentrations. Since many other proteins are known to interact with gold SAMs and the technical requirements for implementation of these experiments are simple, this approach is expected to be very generally applicable to exploring mechanisms of redox proteins and enzymes as well as development of sensors and other redox protein based applications.

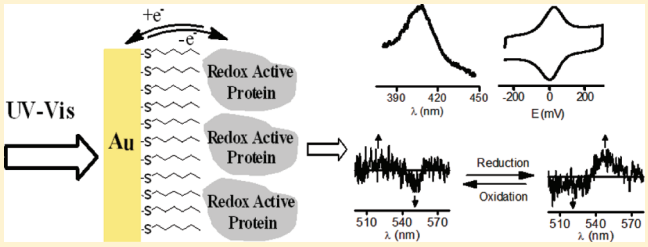

INTRODUCTION

Redox proteins are at the heart of a number of biologically and technologically important processes including respiration and photosynthesis. They currently form the basis for a number of analytic biosensors and are widely investigated for their potential applications in renewable energy technologies.[1,2] Redox proteins consist of protein coordinating one or more redox active cofactors, often prosthetic groups that undergo spectroscopic changes upon oxidation or reduction. Thus, the mechanisms of redox proteins can be explored via both electrochemical and spectroscopic analyses. Although electrochemistry allows precise investigation of the kinetics and thermodynamics of redox reactions, it can be difficult to chemically identify intermediate or product species via electrochemical experiments alone. On the other hand, spectroscopic analyses can be used nondestructively to characterize the chemical features of unknown species but with little control over solution potential or the corresponding redox state of the analyte. The two techniques provide a complementary view of protein function, but correlating independently obtained data is often nontrivial. Thus, spectroelectrochemical methods, those that simultaneously investigate electrochemistry and spectroscopy, provide excellent opportunities to explore mechanisms of redox proteins.[3,4]

Although a number of types of spectroscopies including FTIR, resonance Raman, and EPR have been used to characterize redox proteins, UV−vis is almost certainly the most commonly utilized. Often, the metallocofactors in proteins have strong metal-to-ligand or ligand-to-metal charge transfer transitions in the UV or visible range. Reduction or oxidation of these cofactors results in electronic changes reflected in altered UV−vis spectroscopic features that can be directly correlated to the redox process. Additionally, at a practical level, UV−vis experiments are relatively easy to undertake.

The most widely utilized methodology for protein UV−vis spectroelectrochemistry (SEC) employs a thin layer configuration to optimize diffusion of protein and/or chemical mediator to the working electrode surface, usually a partially transparent Au or Pt mesh.[5] As diffusion by large proteins is relatively slow, these experiments typically employ faster diffusing chemical mediators to relay electrons to protein active sites, thus giving up the ability to precisely control protein potential. Alternatively, they suffer from sluggish

Received: December 21, 2010
Revised: February 22, 2012
Published: February 27, 2012

dx.doi.org/10.1021/la300404r | *Langmuir* 2012, 28, 5861−5871

kinetics, making catalytic observations nearly impossible. Adsorption of a (sub)monolayer of protein to the electrode surface so that electronic exchange is direct rather than via a chemical mediator allows improved control of both electrochemical potential and kinetics. However, the limited quantity of protein present in such an experiment is often too small to be detected in an ordinary transmission spectroscopy experiment. To overcome this challenge, some investigators have utilized layer-by-layer assemblies to build thicker protein layers in contact with electrode surfaces.[6−8] However, this approach trades increased spectroscopic signal for decreased homogeneity, restricted access to active sites, and slower diffusion of substrates or inhibitors within the protein film. Finally, although dozens of proteins have been adsorbed to electrode surfaces and electrochemically characterized using the technique known as protein film electrochemistry (PFE), only two electrode materials have been extensively utilized as working electrodes: pyrolytic edge graphite and self-assembled monolayer (SAM) modified gold.[9,10] Neither of these surfaces is optically transparent, meaning that they cannot be readily utilized in a transmission SEC experiment, and the collection of proteins that have been adsorbed to transparent substrates with maintenance of functionality is very small.[11−14]

To improve sensitivity and spatial resolution, surface-enhanced spectroscopies of various types including Raman,[15] fluorescence,[16] and UV−vis absorption[17] have been described for molecules adsorbed to metallic nanoparticles or thin films. In some cases, reported enhancement factors of up to 14 orders of magnitude have even made single molecule detection possible.[18] Although the mechanism of surface enhancement is still widely debated, resonant transfer of energy from metal surface plasmons to adsorbed molecules is widely hypothesized to account for these phenomena.[19] Like fluorescence resonance energy transfer between two fluorophores, this process requires that the energy of the surface plasmon resonance overlap with the electronic resonance of the adsorbed species. To explore this phenomenon, a number of studies in which nanoparticles with tunable plasmon resonances were synthesized and their interactions with adsorbed species investigated have been reported.[20,21] Furthermore, several studies have shown that interactions between molecular resonances, including those from proteins, and nanoparticle resonances can be detected via localized surface plasmon resonance UV−vis spectroscopy.[22−25]

In this work, we have taken advantage of surface enhancement to develop a sensitive, convenient method for UV−vis spectroelectrochemistry of proteins directly adsorbed to a working electrode at (sub)monolayer coverage. This method allows simultaneously precise control of reduction potential and spectroscopic detection of the species formed. As a working electrode, we have utilized commercial, 100 Å thick, gold films on transparent slides. Thin films of gold (less than ∼15 nm) have good conductivity but show unusual optical properties relative to bulk gold.[26−28] Their high transparency has allowed their utilization as optically transparent electrodes in spectroelectrochemical studies of small molecules including porphyrins.[28] Furthermore, the sensitivity of their surface plasmons to the presence of adsorbates has been widely exploited in sensor technologies.[29,30] The ability to chemically tailor gold surfaces with a wide variety of functional groups via formation of functionalized alkyl thiol SAMs also makes gold a convenient surface for adsorption of a large set of redox active proteins.

Thin films of gold are composed of islands of metal with a relatively large range of sizes such that the surface plasmon resonance spectrum is not a single sharp peak but instead a broad one (see, for example, Figure 3 in ref 28). Thus, chromophores with excitations spanning a broad range of energies should readily interact with the gold surface plasmons. Herein, we demonstrate the ability to adsorb two electrochemically and spectroscopically distinct redox active proteins to transparent, thin gold and simultaneously monitor electrochemical and spectroscopic properties. The two proteins investigated, cytochrome *c* (cyt*C*) and azurin, are well-characterized redox proteins that have been previously investigated via a range of spectroscopic and electrochemical techniques. In addition to spanning two of the most physiologically important classes of redox proteins, hemoproteins and copper proteins, the proteins investigated in this work have electronic absorbances with widely disparate wavelength optima and extinction coefficients, as well as redox transitions spanning a range of more than 400 mV, helping to define the limits of this new technique. Cytochrome *c* contains a redox active heme cofactor with relatively large extinction coefficients (ε can be on the order of 140 000 M^{-1} cm^{-1} for the Soret transition band).[31] The second, azurin, contains a blue copper center, a chromophore with a much lower extinction coefficient (5700 M^{-1} cm^{-1}).[32] The visible absorptions of these two proteins range from 400 to 650 nm and the reduction potentials between 129 and 13 mV vs Ag/AgCl. In this paper, we will demonstrate that, although the quantity of protein adsorbed to the transparent gold surface might be expected to be too small for spectroscopic investigation, both proteins can be interrogated spectroelectrochemically due to spectroscopic enhancement at the transparent gold surface. The amount of protein adsorbed to the gold electrode surface was independently quantified via three different methods: integration of electrochemical signal, AFM imaging of samples, and intensity of spectroscopic response. Excellent agreement is obtained between the electrochemical and AFM data, suggesting that enhancement of the spectroscopic signal of between 8 and 112 times occurs on the gold surface due to resonant energy transfer between the protein chromophores and the gold surface plasmons. Thus, this method can be used to detect proteins spectroscopically at much lower concentrations than expected and will find broad applicability in both mechanistic studies and analytical applications.

MATERIALS AND METHODS

Chemicals. All chemicals were of reagent grade quality and used as received. Ultrapure (Milli-Q systems, resistivity 18.2 MΩ cm^{-1}) water was used throughout.

Azurin Preparation and Purification. *Cell Growth.* Cultures of *E. coli* BL21 (DE3) cells containing a plasmid to express azurin (the WT azurin gene including the periplasmic targeting sequence cloned into the pET9a vector obtained as a gift from Prof. Yi Lu) were grown in LB containing kanamycin (0.5 μL mL^{-1} diluted from of a stock 100 mg mL^{-1}) with shaking (200 rpm) at 37 °C for 8 h. 5 × 1 L cultures (2 × YT with 1 mM $CuNO_3$ and 50 mg L^{-1} kanamycin supplemented) were inoculated from these starter cultures (0.1% inoculum) and were grown with 200 rpm shaking at room temperature for ∼15−24 h or until OD_{600} reached 1. Protein expression was then induced with 75 mg L^{-1} IPTG and growth continued 4−8 h at room temperature, until OD_{600} reached 1.5. Cells were harvested by centrifugation (11000*g* for 10 min), resuspended in a 20% sucrose solution (20% sucrose, 1 mM EDTA, 30 mM Tris), and frozen overnight at −80 °C.

dx.doi.org/10.1021/la300404r | *Langmuir* 2012, 28, 5861−5871

Azurin Purification. Purification of azurin followed a previous procedure[33] with the following modifications. The pH of the isolated periplasmic protein solution was adjusted to 4.1 with 20% acetic acid. The first cation exchange column (CM-sepharose, 25 × 20 cm) was equilibrated with 5 mM ammonium acetate buffer at pH 4.1, and the protein was eluted with a pH gradient of 4.1−6.35. The third column, or second cation exchange column, followed the same pH gradient. The gel-filtration column was excluded from the protocol as it was not found to be necessary. Dialysis was used to exchange the buffer following each chromatographic separation. Concentration of the protein was undertaken only after the final column. Protein purity was verified both by SDS-PAGE (see Figure S4) and the A_{280}/A_{623} ratio via UV−vis spectroscopy (0.53).

Cytochrome *c* Purification. Commercial bovine heart cytochrome *c* (Sigma) was purified as previously described with the following modifications.[34] Protein was dissolved in ice-cold water to a concentration of 1 mg/mL, and a small amount of $K_3Fe(CN)_6$ was added. The protein was applied to a CM-sepharose (GE Healthcare) column pre-equilibrated with 125 mM sodium phosphate buffer at pH 7.5 and eluted with the same. Fractions were collected, pooled, and dialyzed against 5 mM sodium phosphate at a pH of 7.0 before being concentrated to 20 μM in an Amicon Ultra-15 centrifugal filter unit (3000 MWCO, Millipore). Both as-received and purified cytochrome *c* were used in electrochemical experiments without any detectable impact on the electrochemistry. As-received protein was used for spectroscopy and AFM.

Preparation of Thiol Self-Assembled Monolayers (SAMs). *Transparent Au Substrates and Disk Au Electrodes.* Transparent Au substrates (Aldrich, layer thickness 100 Å, referred to throughout the paper as tAu to distinguish it from the more common thicker, nontransparent Au slides) were cut into pieces of 1 in. × 6 mm × 0.7 mm ($L \times W \times$ thickness). The substrates were cleaned by one of two methods. The first is sonicating for 40 min in 20 wt % ethanolamine (Aldrich) in water at ∼50 °C followed by immersion for 20 s in piranha solution (4:1 H_2SO_4:H_2O_2). *Caution: piranha solution is dangerous and should be handled with care.* H_2SO_4 was from EMD Chemicals and H_2O_2 from Sigma. The second, alternative, cleaning method is immersion in an RCA solution (NH_4OH, 30% H_2O_2, and H_2O in a 1:1:5 ratio) for 20 min at 60 °C. The substrates were then washed thoroughly with water and dried under nitrogen. Disk electrodes (2 mm diameter, BASi) were polished successively with 1, 0.3, and 0.05 μm alumina (Buehler) with sonication in water for 2 min between treatments with different particle sizes. The electrodes were cleaned electrochemically by cycling 10 times in 0.1 M H_2SO_4 solution (EMD) between 0.2 and 1.1 V Ag/AgCl (2 mm DRI-REF2 Ag/AgCl reference electrode, World Precision Instruments) as a first stage and then another 15 times with an upper limit of 1.4 V. The electrodes were then treated with piranha solution for 20 s, washed thoroughly with water, and dried under nitrogen.

Assembly of 1-Hexanethiol (HEX) on tAu Substrates and Disk Au Electrodes. SAMs of HEX (Sigma) on either tAu substrates or disk electrodes were prepared by soaking the clean electrodes' surfaces in nitrogen-saturated 6−8 mM ethanolic solutions (EtOH, KOPTEC) of HEX for periods of 24−48 h in a vacuum desiccator at room temperature.

Mixed SAMs of 11-Mercaptoundecanoic Acid (MUA) and 11-Mercapto-1-undecanol (MUOH) on tAu Substrates. Mixed SAMs of MUA and MUOH (both from Sigma) were prepared by immersing the tAu slides in ethanolic solution containing 1 mM MUA and 3 mM MUOH for 48 h in a vacuum desiccator at room temperature. The SAM covered slides were then rinsed with EtOH, sequentially vortexed 3 times in fresh EtOH for 30 s, and dried under nitrogen.

The SAM-modified tAu substrates or disk Au electrodes were immersed in the appropriate protein solutions immediately after preparation.

Formation of Protein Adlayer on Alkylthiol SAM Covered Au Electrodes. *Adsorption of Bovine-Heart Cytochrome c (cytC) on SAM.* Au substrates were incubated in a solution of 20 μM cytC for ∼4 h at 4 °C (pH 7, 5 mM potassium phosphate buffer). The concentration of cytC was determined from the optical absorption at 410 nm using ε = 106 100 M^{-1} cm^{-1}.[35]

Adsorption of Azurin on SAM. Both HEX-modified tAu substrates and disk Au electrodes were incubated in a solution of 120 μM azurin for ∼1 h at 4 °C (pH 4.1, 100 mM Na_2SO_4 and 50 mM NH_4OAc, each from Sigma). The concentration of azurin was determined by its optical absorption at 628 nm using ε = 5700 M^{-1} cm^{-1}.[32]

Shortly after the assembly of proteins, the electrodes were rinsed with the corresponding working buffers and used for the experimental examination while fresh.

Electrochemical and Spectroelectrochemical Measurements. Electrochemical measurements were performed using CV50W (BAS) or PGSTAT 12 Autolab (Ecochemie) potentiostats. Data were collected using the BAS dedicated software or the GPES software package (Ecochemie) relevant to the potentiostat used. Spectroscopic data were collected using a Perkin-Elmer Lambda 650 UV−vis spectrophotometer. The electrochemical interrogation of transparent Au substrates was carried out in a specially designed spectroelectrochemical cell (Figure S5) that consists of a Teflon cap housing the tAu substrates as the working electrode, a Ag/AgCl reference electrode (2 mm diameter, Driref-2, World Precision Instruments), and a platinum wire as the counter electrode. The Teflon holder was inserted into a standard optical cuvette that contained the buffered electrolyte solution. This setup provides a fixed geometry for the electrodes in which the tAu substrate is situated vertically and distant from the other electrodes to avoid short-circuit connections. A small rounded aperture (1.2 mm diameter) in the Teflon holder allows the insertion of a tube by which the composition of dissolved gases can be controlled. The volume of the working buffer solution within the cell covered a typical geometric area of ∼0.72 cm^2 of the working Au electrode. Prior to measuring, the cell was purged with N_2 for 20 min. During data collection, the tube was set slightly above the solution to maintain anaerobic conditions throughout without disturbing the measurement. Combined optical-absorption and electrochemical measurements were carried out at 22 °C. For electrochemical analysis at 4 °C, the cell was situated in an exterior cuvette holder that was connected to a circulating chiller (VWR). Kinetic analysis of the electrochemical data was done using the Windows-based freeware Jellyfit.[36]

pH Measurements. The stability of the buffered conditions was assessed by measuring the pH value inside the spectroelectrochemical cell before and after each measurement using a 2 mm pH electrode (HI1093, HANNA Instruments).

Atomic Force Microscopy (AFM). For the AFM measurements, an MFP3D-Bio AFM from Asylum Research was used. To reduce thermal drift during the scans, the temperature of the sample was kept at 26 °C using a dish heater from Asylum Research. For tapping mode in air and lithography, AFM probes with a resonance frequency of about 310 kHz and a spring constant of about 20 N m^{-1} (PointProbePlus NHC, Nanosensors) were used. For lithography, the probe was brought into contact with the surface. No or little force was applied to the probe, so capillary forces on the order of 1 nN dominate the force between the probe and the surface. Measurements were performed on bare tAu and on protein adsorbed substrates that were prepared in the same way as for the electrochemical measurements. Before imaging, the protein adsorbed substrates were left in protein-free buffer for 2−10 min to ensure the removal of loosely bound proteins and then imaged dry after removal from the buffer without any further washing steps in the case of azurin and cytC. For image analysis, SPIP version 4.5.5 (Image Metrology, Denmark) and the Asylum Research software version 090909.1425 based on IgorPRO version 6.12 (Wavemetrics, Portland, OR) were used.

RESULTS AND DISCUSSION

To demonstrate the ability to monitor both electrochemical and spectroscopic properties of proteins adsorbed to SAMs on transparent gold (designated tAu throughout to distinguish it

dx.doi.org/10.1021/la300404r | *Langmuir* 2012, 28, 5861−5871

from thick, nontransparent substrates), two different redox proteins have been investigated: (1) cytochrome *c* (cytC), a well-known redox protein that has been well-characterized on SAM-modified crystalline Au electrodes, and (2) the blue copper protein azurin, a redox protein with a much lower extinction coefficient for its visible transition than the hemoprotein cytC.[37] Results arising from each of these proteins will be considered in turn below as proof of the utility of this platform for protein spectroelectrochemical investigation.

Electrochemical and Spectroelectrochemical Characterization of cytC Adsorbed onto a Mixed Alkanethiol SAM Modified tAu Substrate. The redox-active heme protein cytC has been shown to adsorb, with retention of redox functionality, to a number of electrode surfaces.[9,12,38−42] In particular, direct electrochemical studies of cytC on gold surfaces have utilized carboxy-terminated self-assembled monolayers (SAMs) to promote stable, functional interactions. In this type of assembly, surface lysines of the protein are thought to mediate electrostatic interactions with the SAM. In addition, some reports have shown that dilution of a carboxylic acid-terminated SAM with a primary alcohol can improve the electroactive coverage or interfacial electron transfer rate of adsorbed cytC.[9,43] Thus, in this work, we have utilized a mixed SAM (1:3 ratio) of MUA and MUOH to facilitate adsorption of bovine heart cytC to commercially prepared, 100 Å thick tAu substrates and characterized the resulting electrochemistry and UV−vis spectroscopy. The entire assembly will be referred to as cytC/MUA_MUOH/tAu, and analogous protein/SAM component/substrate nomenclature will also be used throughout the paper to refer to other protein−electrode combinations.

Figure 1a shows a representative cyclic voltammogram arising from cytC/MUA_MUOH/tAu, and Table 1 summarizes the electrochemical parameters (an average of three independent trials). Clearly resolved peaks centered at 39 ± 11 mV (vs Ag/AgCl) are observed. This reduction potential is very similar to that reported for other cytC assemblies on electrodes as well as cytC in solution,[9,41] and the peaks are not present when protein is omitted from the experiment. Furthermore, the dependence of the peak positions on scan rate is linear, indicating that the signals arise from an adsorbed, as opposed to diffusing, redox active species (Figure 2a). The signals are highly symmetric and display very little peak separation, 29 ± 4 mV, at low potential scan rates. This suggests a nearly ideal, reversible redox couple gives rise to the signal.[44] Furthermore, fast scan cyclic voltammetric analysis demonstrates that the kinetics of the gold/protein electron exchange is relatively fast. Using a Butler−Volmer kinetic model[44,45] to fit data such as that shown in Figure 2b yields a k^0_{ET} value of 26 ± 15 s^{-1}. A control experiment utilizing the same MUA_MUOH SAM on a gold disk electrode produced a k^0_{ET} value of 63 s^{-1}. Davis and co-workers have reported a similar value of 53 ± 4 s^{-1} measured for cytC adsorbed on a SAM produced from a 2:3 mixture of MUA_MUOH on an ordinary, Au electrode.[9] Thus, we conclude that cytC adsorbs to the SAM covered tAu with retention of its native redox functionality and is able to exchange electrons as efficiently with the underlying tAu substrate as with ordinary crystalline Au electrodes.

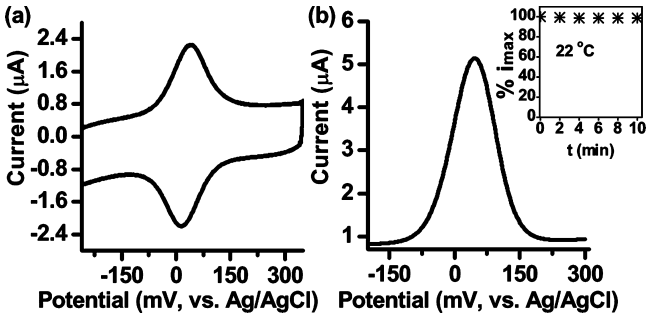

Figure 1. (a) Cyclic voltammogram and (b) square wave voltammogram from cytC/MUA_MUOH/tAu in an anaerobic solution of 5 mM potassium phosphate (pH 7). Cyclic voltammetry was recorded at 250 mV s^{-1} and 22 °C. Square wave voltammetry utilized the following parameters: amplitude 25 mV, frequency 15 Hz, and potential step 2 mV. The inset of panel b shows the time-dependent decay of the peak current (normalized values) at 22 °C.

Since both the density and stability of SAMs on tAu may not be identical to that on crystalline Au, we determined both how much protein was adsorbed on the electrode and the stability of the resulting assembly. Control electrochemical experiments demonstrated that only a negligible quantity of potassium ferricyanide was able to penetrate the SAM to interact with the tAu suggesting that the SAM itself is relatively well packed (Figure S1). The electroactive coverage of protein (Γ_{ea}) on a surface can be determined from the equation

$$\Gamma_{ea} = \frac{A_{CV}}{nF\nu A_{elec}} \quad (1)$$

in which A_{CV} is the area under the observed cyclic voltammetry peak, n is the number of electrons transferred in the redox process (assumed to be one for cytC), F is Faraday's constant, A_{elec} is the geometrical electrode area, and ν is the potential scan rate. The average electroactive coverage observed for cytC/MUA_MUOH/tAu was 6.7 pmol cm^{-2}. This value is about 1.8-fold lower than the 17 pmol cm^{-2} expected for dense monolayer coverage of a spherical protein with a cross-sectional area of 10 nm^2, an approximation of cytC based on the X-ray crystal structure.[41,46] However, within error, we observe the same coverage (5.85 pmol cm^{-2}) for a SAM of the same composition on an ordinary gold disk electrode. Near monolayer coverage has been reported for electrostatic adsorption of cytC to carboxylic acid-terminated SAMs. However, our observed coverage is very similar to values such as 7.2 ± 4.8 pmol cm^{-2} reported for cytC covalently attached via an amide linkage to a carboxylic acid SAM at thicker, nontransparent gold surfaces (see ref 41 and references therein). It is natural to ask whether all of the adsorbed protein is oriented in a homogeneous configuration on the electrode surface. In answer to this question, we consider the widths of the voltammetric peaks. The peak width at half-maximum is 105 ± 2 mV, noticeably larger than the 90 mV theoretically predicted[44] but comparable to what has been previously observed for adsorbed cytC. This suggests that the protein is adsorbed in a distribution of orientations on the electrode surface very much like that seen in other studies on thicker gold surfaces. Considering there are 15 lysines distributed over the surface of cytC, each of which could facilitate interactions with the SAM, a range of protein orientations is not surprising.

The electrochemical signals arising from cytC/MUA_MUOH/tAu are remarkably stable. The more sensitive square wave voltammetric technique was utilized to quantify the decay of electroactive coverage as shown in Figure 1b. The area of the peak was monitored over a period of 10 min, during

dx.doi.org/10.1021/la300404r | Langmuir 2012, 28, 5861−5871

Table 1. Electrochemical and Spectroscopic Parameters of cytC Adsorbed on MUA_MUOH Modified Au Electrodes and of Azurin Adsorbed on HEX Modified Au Electrodes[a]

	$E_{1/2}$ (mV vs Ag/AgCl)[a]	surface coverage[b,c] (Γ, pmol cm^{-2}) anodic, cathodic	decay of electrochemical activity (% min^{-1}) 22 °C	λ_{max} (nm)	k^0_{ET} (s^{-1})	ΔE_p (mV)[d]	fwhm (mV)[d]
cytC/MUA_MUOH/tAu	39 ± 11	7.1 ± 3.3, 6.3 ± 2.5	0.08	408 ± 2	26 ± 15	29 ± 4	105 ± 2
cytC/MUA_MUOH (disk electrode)	10.6 ± 1.2	6.0 ± 3.6, 5.7 ± 3.7	ND[e]	ND	ND	ND	ND
Az/HEX/tAu	132 ± 3	4.7 ± 0.6, 4.6 ± 0.3	4.1	602 ± 7	344 ± 252	19 ± 6	102 ± 4
Az/Hex (disk electrode)	151 ± 25	12.9 ± 0.9, 13.3 ± 0.4	ND	ND	ND	ND	ND

[a]All parameters (except decay of electrochemical activity) are an average of three independent experiments, and the uncertainties are one standard deviation. [b]Evaluated by using eq 1 for data at 250 mV s^{-1}.[47] A typical value of the tAu working electrode area was 0.72 cm^2. [c]Anodic: calculated according to the area of the anodic peak; cathodic: calculated according to the area of the cathodic peak. [d]Data correspond to a scan rate of 250 mV s^{-1}. [e]ND indicates not determined.

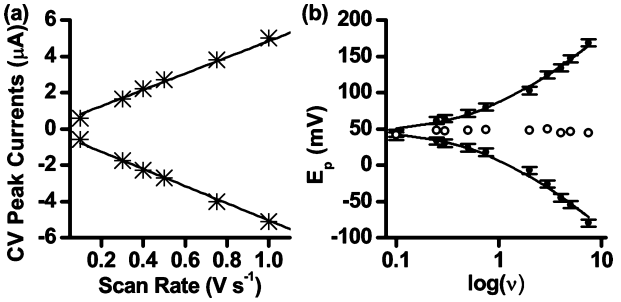

Figure 2. (a) Dependence of cyclic voltammetric peak current on scan rate for cytC/MUA_MUOH/tAu. The solid lines show linear fits to the data. A correlation coefficient (R^2) of 0.97 was obtained for both the anodic and cathodic data. (b) Dependence of cytC/MUA_MUOH/tAu cyclic voltammetric peak position on the scan rate (measured from 0.1 to 7.5 V s^{-1}). The experimental data (black filled circles) were fitted to a Butler–Volmer kinetic model (solid lines) with a k^0_{ET} value of 15.9 s^{-1} at 90% confidence level. The empty circles are the calculated average reduction potential. The error bars correspond to an experimental error of ±5 mV that was used as the boundary for the fitting process. Temperature, pH, and buffer conditions are as defined in Figure 1.

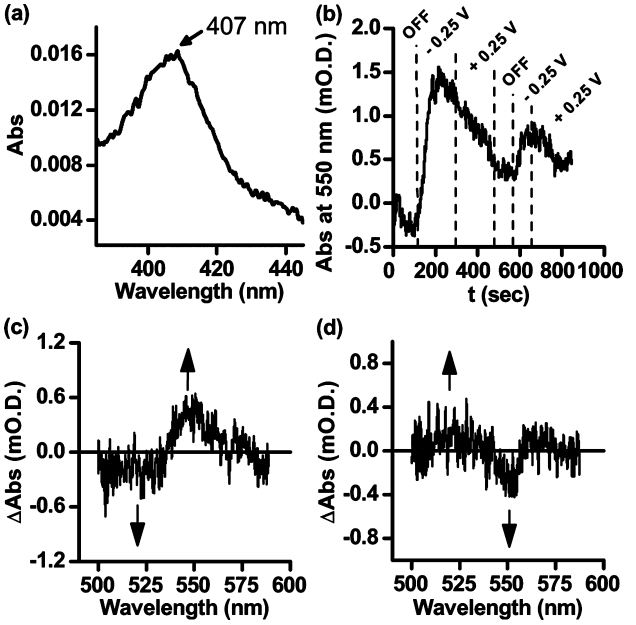

Figure 3. (a) Absorption spectrum of cytC/MUA_MUOH/tAu in the characteristic Soret region of hemes. (b) Absorbance at 550 nm as a function of time under electrochemical potential control. Dotted lines indicate the times at which the potential was changed, and each time period is labeled with the potential applied during that interval. The open-circuit potential is designated as "off". (c) Difference absorption spectrum resulting from subtraction of the spectrum obtained under open-circuit conditions from one obtained after a 4 min application of −250 mV. (d) Absorbance difference spectrum resulting from subtraction of the reduced species spectrum obtained in panel C from that obtained after oxidation at +250 mV for 4 min. The experimental conditions are as in Figure 1.

which the film was electrochemically probed once every 60 s (Figure 1b, inset), and the rate of decay was estimated at 0.08% min^{-1}. As a control, the stability of electrochemical signals arising from cytC adsorbed to the same SAM assembled on a gold, disk electrode was measured. The control showed practically no decay of the protein signal over 30 min. This stability enables thorough and reliable investigation of physical, electrochemical, and structural properties of the protein adlayers. Preservation of the adlayer integrity is especially important when the sampling duration of analysis can stretch over tens of minutes as in the case of the spectroscopic investigation presented below.

The transparency of tAu allows simultaneously strict potential control of the protein film, as demonstrated by the electrochemical signals above, and detection of redox state changes via UV–vis spectroscopy. In an ordinary transmission mode spectroscopy experiment, the characteristic Soret transition band of cytC could clearly be observed at 408 nm in the absorbance spectrum obtained through the cytC/MUA_MUOH/tAu assembly (Figure 3a). Furthermore, as we demonstrate below, absorption changes in the Q-transition band region could be used to monitor the redox state of the adsorbed protein on the tAu surface. Figure 3b shows that application of a reducing potential, −250 mV, causes an immediate increase in absorbance at 550 nm, the maximum of the Q-transition band of reduced cytC. The absorbance change saturates after ∼100 s, indicating that potential control of the protein redox state is relatively fast. Switching the applied potential to +250 mV then causes a similar decrease in absorbance corresponding to oxidation of the protein and demonstrating that the process is reversible. Importantly, the entire cycle can be repeated, indicating that there is truly potential control of the protein's redox state. In the second cycle, the amplitude of the absorbance changes is much smaller, suggesting that the protein is desorbing from the surface under constant potential application. Figure 3c,d shows the difference spectra from an analogous experiment. First, a spectrum under open cell potential was obtained. Then a reducing potential was applied for 4 min, and a second spectrum was obtained. Figure

dx.doi.org/10.1021/la300404r | Langmuir 2012, 28, 5861–5871

3c shows the difference spectrum resulting from the reduced minus the open cell spectrum. As expected, there is a clear increase in absorbance at 550 nm corresponding to reduction of the heme. Figure 3d demonstrates that the protein can then be reoxidized. The sample was oxidized at +250 mV for 4 min, and another spectrum was obtained. Figure 3d shows the oxidized minus reduced spectrum. A clear decrease in absorbance at 550 nm demonstrates reoxidation of the heme. These spectra conclusively show the ability to control reversibly the oxidation state of the adsorbed cytC and monitor the changes spectroscopically through the underlying tAu layer.

It is interesting to compare the magnitude of the absorbance measured to that expected based on the electroactive coverage of protein, 6.7 pmol cm^{-2}. The absorbance for an adsorbed layer can be determined according to the following equation, an expression of the Beer–Lambert law:

$$\text{Abs} \times 10^{-3} = \varepsilon_{\text{adlayer}} \times \Gamma_{\text{adlayer}} \quad (2)$$

in which Abs is the measured absorbance, $\varepsilon_{\text{adlayer}}$ is the extinction coefficient for the adsorbed protein (M^{-1} cm^{-1}), and Γ_{adlayer} again represents coverage (mol cm^{-2}).[48] For oxidized cytC, ε_{410} in solution for the Soret transition band is 106 100 M^{-1} cm^{-1},[35] and thus, using the electroactive coverage, we predict an absorbance of 0.000 71. The observed value of 0.016 is ~23 times higher than expected. Similarly, for the reduced state using the Q-transition band ε_{550} of 27 700 M^{-1} cm^{-1} a signal enhancement of ~8 times over what was expected is observed. In both cases, the observed spectroscopic signal is approximately an order of magnitude greater than what would be expected for the adsorbed quantity of protein determined electrochemically. This then begs the question, is there a substantial quantity of protein participating in the spectroscopic experiment that is unobserved electrochemically, i.e. not in fast electronic communication with the tAu surface? In light of the fact that the redox state of the protein can be rapidly changed by application of a potential to the tAu surface, we do not believe this to be the case. Furthermore, as we will show below, a similar enhancement is observed for the protein azurin adsorbed to tAu. Additionally, AFM imaging of both proteins on tAu suggests that only a submonolayer of protein is on the surface. With this in mind, we will return to a discussion of the enhancement of the spectroscopy below.

Electrochemical and Spectroscopic Characterization of Azurin Adsorbed onto Transparent Au Substrates. To establish the limits of the utility of tAu for protein spectroelectrochemical investigations, we have also undertaken experiments with the blue copper protein azurin from *Pseudomonas aeruginosa*. Azurin (14.6 kDa) is well-known to adsorb to pyrolytic graphite or to alkanethiol modified Au surfaces in an electroactive configuration capable of fast electron exchange with the solid surface,[37,47,49−55] and in solution, a characteristic ligand-to-metal charge transfer band is observed in the optical spectrum at 628 nm.[32,56] The extinction coefficient for this transition, 5700 M^{-1} cm^{-1}, is almost 2 orders of magnitude lower than that of the Soret transition band of hemes, making it significantly more challenging to investigate this protein spectroscopically in a thin film configuration.

Figure 4 shows that azurin can also functionally adsorb to hexanethiol SAM (HEX) modified tAu (Az/HEX/tAu). The electrochemical parameters of the Az/HEX/tAu system are summarized in Table 1. The cyclic voltammograms observed with this tAu platform are very similar to the best of those

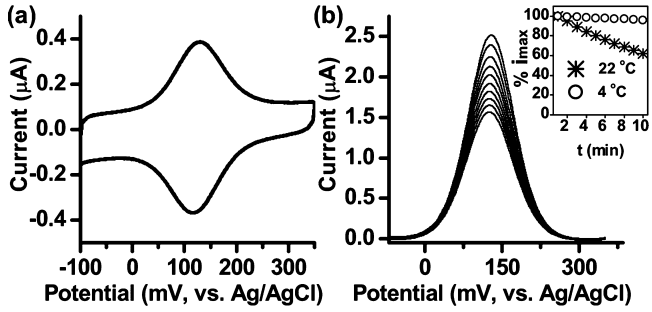

Figure 4. Cyclic and square wave voltammograms of Az/HEX/tAu in an anaerobic solution of 100 mM Na_2SO_4, 50 mM NH_4OAc (pH 4.1): (a) cyclic voltammetry was recorded at 100 mV s^{-1} at 22 °C; (b) square wave voltammetry was performed using the following scan parameters: SW amplitude 25 mV, frequency 15 Hz, and potential step 2 mV. The inset shows the time-dependent decay of the peak current (normalized values) at 22 °C (stars) and 4 °C (empty circles). See Figure S2 for SW data at 4 °C.

observed for azurin on ordinary Au electrodes.[37,50,54,57] As expected, a reversible pair of highly symmetric peaks, with very little peak separation (19 ± 6 mV), centered at 132 ± 3 mV (vs Ag/AgCl) was detected. The reduction potential is very similar to both values measured for azurin in solution via potentiometric titrations[32] and potentials measured via PFE on nontransparent electrodes.[47,50,58] Additionally, the low peak separation suggests that interfacial exchange of electrons between the azurin and tAu is relatively facile. The peak width at half-maximum, 102 ± 4 mV, is larger than theoretically predicted for a Nernstian, one-electron process[44] but comparable to what has previously been observed in PFE experiments with azurin.[37,47] Figure 5 shows a "trumpet plot",

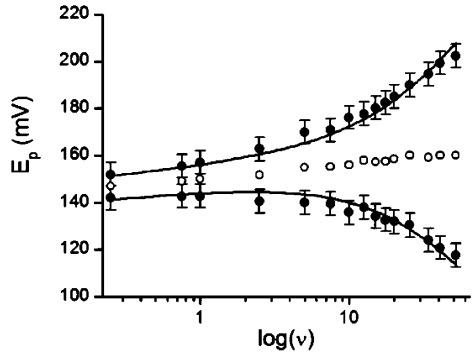

Figure 5. Dependence of Az/HEX/tAu potential peak position on the scan rate (measured from 0.25 to 52 V s^{-1}). The experimental data (black filled circles) were fit to a Butler–Volmer kinetic model (solid lines) with a k^0_{ET} value of 621.6 s^{-1} at 95% confidence level. The empty circles show the average reduction potential which remains relatively constant over the scan rate range of the experiment. The error bars correspond to an experimental error of ±5 mV used as boundaries for the fitting process.

the current peak potentials as a function of the scan rate. The standard electron transfer rate at zero overpotential, k^0_{ET}, was estimated to be 344 ± 252 s^{-1}. Previous kinetic analyses for azurin adsorbed on Au films have yielded values between 150 and 165 s^{-1} for azurin directly bound through a surface cysteine residue to the Au surface[52] and values between 20 and 140 s^{-1} for azurin monolayers adsorbed onto alkanethiol-modified Au substrates and nanoparticles.[54,56] Taking uncertainty into

dx.doi.org/10.1021/la300404r | Langmuir 2012, 28, 5861−5871

account, the value reported here is consistent with what has been previously reported for azurin monolayers on SAM covered Au. Additionally, we measured a similar value of k^0_{ET} = 427 s^{-1} for the Az/HEX on a gold disk electrode.

As described for cytC (eq 1), the electroactive coverage of protein can be determined from the areas under voltammetric peaks. The average coverage of azurin in the Az/HEX/tAu assembly was 4.65 pmol cm^{-2}. A control experiment in which azurin was adsorbed to a hexanethiol monolayer on a disk gold electrode yielded a coverage of 13.1 pmol cm^{-2}, a value ~2.8 times higher than that observed on thin gold. However, we note that others have reported electroactive coverages on the order of 6 pmol cm^{-2} for azurin adsorbed to a hexanethiol monolayer on gold.[37,50] As for cytC, the measured electroactive coverage for azurin is smaller than what would be expected for a densely packed monolayer, 24 pmol cm^{-2} assuming a spherical radius of 1.5 nm.[47] Remarkably, AFM imaging (see below) of the tAu assembly detects a nearly identical quantity of protein on the electrode surface, indicating that the overwhelming majority of the adsorbed protein is in electrochemical contact with the tAu electrode.

Since the functional stability of adsorbed proteins on electrode surfaces can be a limiting factor in PFE experiments, square wave voltammetry has again been used to quantitatively characterize the stability of the Az/HEX/tAu assembly. The inset in Figure 4b shows the time-dependent decay of the electrochemical activity at 22 and 4 °C. The decay rate was evaluated by linear fitting of the data (Table 1) establishing a value of 4.1% min^{-1} at 22 °C and 0.4% min^{-1} at 4 °C. Interestingly, significant stabilization of the adlayer was observed upon lowering the temperature to 4 °C; the decay rate decreased by ~90% (from 4.1 to 0.4% min^{-1}). These values are very similar to those obtained in stability measurements of alkanethiol SAMs on Au, suggesting that the major cause of loss of electrochemical activity is decay of the SAM as opposed to denaturation or desorption of the protein.[57]

Although the extinction coefficient for azurin is more than an order of magnitude lower than that of cytC and we might expect that optical signals for azurin would be well below detection limits, Figure 6 demonstrates that features attributable to the adsorbed azurin can be observed in the UV–vis spectrum of Az/HEX/tAu (blue line). Spectra for the adsorbed protein were obtained by subtracting from the collected data the spectrum of the HEX-covered tAu substrate obtained prior to incubation with azurin. Utilization of the spectrum of bare tAu as the background for subtraction also yielded similar results. Two additional SAMs, 1-decanethiol (DEC) and 1,6-hexanedithiol (HDT), were also investigated (see Figure S3), and observed maxima for the adsorbed protein in these systems ranged between 600 and 650 nm. For comparison, the spectrum of azurin in solution is superimposed (black line). The characteristic ligand-to-metal charge transfer band involving mainly the $d_{x^2-y^2}$ orbital on the Cu and a 3p orbital of the Cys112 sulfur is centered at 628 nm.[56] In all cases, the characteristic shape of the ligand-to-metal charge transfer is clearly observed in the spectra of the adsorbed azurin on tAu. As for cytC, the observed optical intensities for adsorbed azurin are significantly higher than what would be expected when applying a Beer–Lambert relation according to eq 2. As will be demonstrated below, the total coverage of protein molecules determined by AFM, $\Gamma_{adlayer}$, coincides with the electroactive coverage of azurin molecules. Hence, using 4.65 pmol cm^{-2} for $\Gamma_{adlayer}$ and the simplified assumption that the extinction coefficient of the adsorbed species, $\varepsilon_{adlayer}$, is similar to that of azurin in solution (5700 M^{-1} cm^{-2} for azurin at 628 nm), one should expect an absorption intensity that is as low as 0.027 mOD, ~2 orders of magnitude lower than detected. This gives rise to an apparent absorption intensity enhancement of ~112-fold for the adsorbed azurin species. Surface-induced absorption enhancement is a well-known phenomenon in general and is widely applicable in various forms of gold-based materials. Before discussing further and assigning any kind of enhancement phenomena to the observed spectra of the Az/HEX/tAu system, it is essential to characterize the morphology of the adsorbed protein at the tAu surface and verify that the UV–vis absorption signal does not originate from a multilayer structure in which most of the outer layers are nonelectroactive azurin adlayers. The following section presents an AFM characterization of the protein/tAu systems and demonstrates that there is not more protein present on the surface than accounted for by the electrochemical measurements.

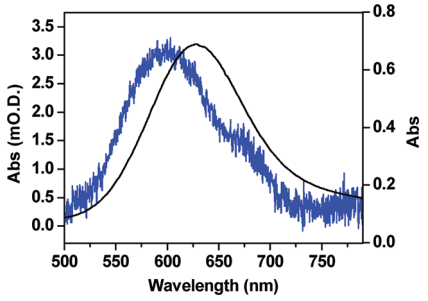

Figure 6. Optical absorption spectra of Az/HEX/tAu (blue line, corresponding to the left ordinate) together with a superimposed spectrum of 120 μM of dissolved azurin (black line, corresponding to the right ordinate). Solvent: anaerobic 100 mM Na_2SO_4, 50 mM NH_4OAc (pH 4.1) at 22 °C.

AFM Characterization. To evaluate the coverage of the electrodes with protein, the bare tAu substrates were imaged via AFM to identify the morphology of the surface. Electrodes incubated with protein were then compared with this data. The transparent gold layer alone exhibits a grain structure with an rms roughness of 0.6 nm (Figure 7a).

cytC/MUA_MUOH/tAu. AFM images of cytC covered electrodes revealed a relatively densely packed surface without obvious background features corresponding to the morphology of the bare gold surface (Figure 7b). Therefore, we performed lithography to establish the height of the adsorbed protein layer. The thickness of the protein layer was between 1.3 and 2 nm. This is similar to or slightly less than the crystallographically determined size of cytC: 3.56 nm (1.78 nm hydrodynamic radius), and the results are similar to those obtained by Nakano and co-workers for cytC adsorbed on MUA modified Au films (the exact thickness of the gold was not identified in that work and thus cannot be used for comparison).[41] The apparent shrinkage of cytC on the tAu can be explained in two ways. First, the protein may compact when dehydrated, the condition of the AFM experiment. Second, the protein height may be slightly underestimated due to difficulty accounting for the underlying gold surface roughness. Figure 7 shows the AFM height image (c) after lithography and the average cross section for the scraped area (d). We have estimated the coverage by determining the volume from an AFM height image (Figure 7b) above a threshold that is set to be at the level of holes in the protein surface, which are

dx.doi.org/10.1021/la300404r | Langmuir 2012, 28, 5861–5871

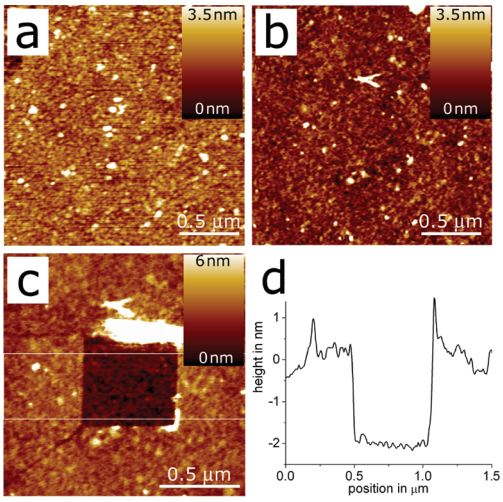

Figure 7. (a) Tapping mode AFM image of the bare tAu. The topography shows a grain structure with an rms roughness of 0.6 nm. (b) Tapping mode AFM height image of a cytC slide. (c) Tapping after lithography. (d) Average cross section through the scraped area shown in (c).

assumed to be the gold background. Note this method will account for all protein imaged including any high, multilayer clusters. The error in the estimation of the volume is governed by the uncertainty in the background level and errors due to the finite size of the AFM tip. The error is assumed to be as big as 50%. A molar coverage for cytC of 7 pmol cm^{-2} was calculated by dividing the volume by the size of protein. This value is in good agreement with the 6.7 pmol cm^{-2} detected electrochemically.

Az/HEX/tAu. Images of Az/HEX/tAu were particularly sensitive to preparation and handling, and images with a range of protein densities on the surface were obtained. Figure 8 shows a typical image of Az/HEX/tAu sample that was measured immediately after preparation under the identical conditions used for electrochemistry and spectroscopy. Comparison of the surface before and after incubation with protein makes clear that introduction of the protein results in a dramatic change in the surface topography (Figure 8a,b). After incubation with protein, clearly defined features with dimensions expected for single proteins or small clusters are observed above the gold background. To evaluate the coverage, standard AFM grain analysis was performed. From the AFM height image, the shape of the AFM tip was estimated (built-in function of SPIP),[59,60] and the image was deconvoluted with this shape (Figure 8b).

Individual features with heights between 3 and 15 nm were distinguished above the background tAu substrate, and a histogram of particle heights is shown in Figure 8e. The smaller dots can be attributed to single proteins on the surface, while the larger dots correspond to aggregates of small numbers of proteins. The isolation of the proteins or protein clusters suggests that the adsorbed protein forms a noncontinuous, submonolayer. Furthermore, approximating azurin as a sphere of radius 1.5 nm,[47] for any particular protein particle, between one and three layers of protein were adsorbed to the tAu surface. To quantitatively determine the coverage of proteins on the tAu surface, particles were detected using the height threshold method with prior equalization of the background level (Figure 8c). The phase image (Figure 8d), in which the

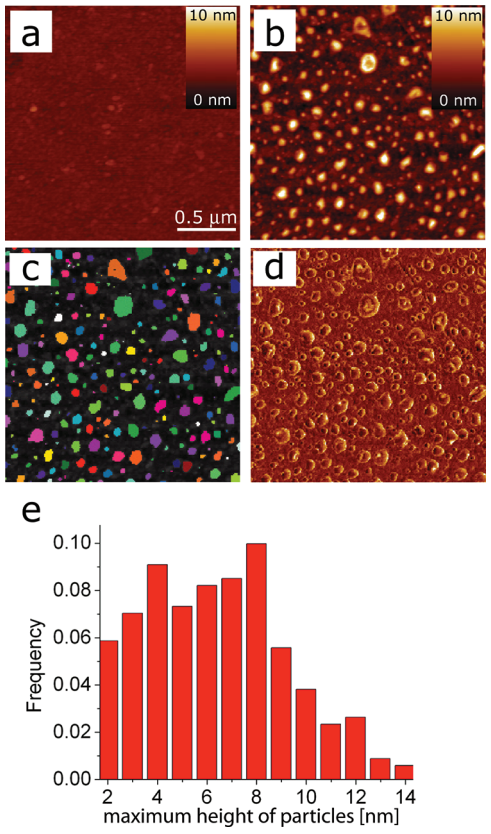

Figure 8. (a) Tapping mode image of the bare tAu. Same data as Figure 7a but rescaled. (b) Tapping mode AFM height image of an Az/HEX/tAu slide. The topography has been deconvolved with an estimated tip shape to account for tip-induced artifacts. (c) Particle analysis results. Each detected particle is false colored individually to allow for visual inspection of the quality of the analysis. (d) Phase image matching panels b and c. The tapping mode AFM phase image reveals a clear contrast between the surface and the adsorbed proteins allowing evaluation of the quality of the particle analysis (e) Distribution of maximum height values from the azurin image in panel b. Small clusters of protein up to 15 nm in height as well as single proteins with heights up to 5 nm can be distinguished from the graph. The height values are measured with respect to the threshold level that was used for particle analysis.

proteins are nicely distinguished from the background, confirms the quality of the detection method. The volumes of individually detected particles were summed to determine total occupied volume. Then the amount of protein on the surface was found to be in a range of 3.02−5.8 pmol cm^{-2},[47] in good agreement with the 4.65 pmol cm^{-2} determined electrochemically.

■ CONCLUDING REMARKS

We have utilized for the first time transparent gold as a substrate for adsorption of redox proteins and investigation by spectroelectrochemistry. This approach combines the simplicity of forming robust thiol SAMs on Au surfaces with the high conductivity and transparency of a thin Au substrate that is commercially available. Adsorption of proteins to electrode surfaces and investigation via unmediated electrochemistry allows better kinetics and more precise electrochemical potential control than either diffusing or mediated electrochemistry. Thus, it is important that we have shown that utilization of a transparent gold substrate does not sacrifice

dx.doi.org/10.1021/la300404r | *Langmuir* 2012, 28, 5861−5871

anything in terms of the quality of the electrochemical investigation relative to unmediated adsorbed protein electrochemisty at such surfaces as bulk gold and pyrolytic graphite. The electrochemical responses of both of the proteins investigated are comparable to those previously observed on ordinary disk gold electrodes. Surprisingly, the spectroscopic signatures of each of these proteins can also be observed through the semitransparent, thin gold in an ordinary transmission mode experiment, and they are very similar to what has been observed in solution. Although one might initially expect that the spectroscopy is made possible by adsorption of a number of layers on the electrode surface, many of which may not be in electronic contact with the underlying gold and thus eliminated the advantage of precise potential control of the protein film, AFM imaging conclusively demonstrates that both of the proteins adsorb at submonolayer coverage, and multilayer assemblies have not been formed. Furthermore, in the case of cyt*C*, potentiostatic control of the gold surface can induce the expected changes in the heme spectroscopy demonstrating that the spectroscopically observable protein is also able to exchange electrons with the gold surface on a reasonably fast time scale. For both proteins investigated, there is an apparent contradiction between the quantity of protein on the electrode surface and the observed spectroscopic signal; i.e., the spectroscopic signal is much larger than would be expected for the quantity of adsorbed protein. This can be explained by surface enhancement due to interactions of the proteins' electronic transitions with the gold surface plasmon. The relatively broad surface plasmon of the tAu film is able to interact with both the Soret (410 nm) and Q-transition bands (reduced, 550 nm) of the heme in cyt*C*, causing apparent enhancements of ∼23 and ∼8 times, respectively. Similarly, the charge transfer band of azurin (628 nm) was enhanced 112-fold. The variation of the observed maximum for azurin over a range of 50 nm between experiments, a range that would be inexplicable in a classical solution UV−vis experiment, may also be indirect evidence for a surface enhanced effect. As already described for localized surface plasmon spectroscopy,[25] the interaction between the gold plasmon and an adsorbed chromophore should be wavelength dependent, leading to different enhancement values for different wavelengths. These interactions should be extremely sensitive to the precise orientation and redox state of the adsorbed species, and subtle heterogeneity between experiments could lead to large changes in the observed optical maximum. Thus, in the experiments with azurin, heterogeneity in the orientation of the adsorbed azurin may be sufficient to cause relatively variable optical maxima. Additionally, optical enhancement should also be very sensitive to the distance between the chromophore and the gold surface, a relatively difficult to define value since the transparent gold layer is rough. It may be possible to systematically investigate the impact of protein orientation on the observed optical enhancement by investigating the spectroscopy of a single protein adsorbed to a number of different SAMs. Azurin should be an ideal protein for such studies since it can adsorb to surfaces through either a hydrophobic patch or a surface cysteine, and we have already seen that the wavelength maximum can be significantly altered by experimental conditions. This will be a topic for future investigation.

Although the surface enhancements observed in this work are modest relative to some reported for Raman spectroscopy, surprisingly, they are sufficient to allow spectroscopic observation of proteins in a system with precise and fast electrochemical potential control. This should open up new opportunities both for exploration of redox protein mechanisms and development of analytical tools based on redox proteins. Finally, this platform also presents a new opportunity for investigations into the mechanism of surface enhancement of electronic transitions more generally.

■ ASSOCIATED CONTENT

Ⓢ Supporting Information

Additional electrochemical and spectroscopic data; schematic of spectroelectrochemical cell. This material is available free of charge via the Internet at http://pubs.acs.org.

■ AUTHOR INFORMATION

Corresponding Author

*E-mail: jonesak@asu.edu; Tel: 480-965-0356; Fax: 480-965-2747.

Notes

The authors declare no competing financial interest.

■ ACKNOWLEDGMENTS

Prof. Yi Lu is thanked for providing the plasmid for overexpression of azurin. C.L.M. was supported by the Science Foundation Arizona as a Graduate Research Fellow. A.K.J. and C.L.M. are supported as part of the Center for Bio-Inspired Solar Fuel Production, an Energy Frontier Research Center funded by the US Department of Energy, Office of Science, Office of Basic Energy Sciences, under Award DE-SC0001016. Additionally, financial support for this work was provided by Arizona State University.

■ REFERENCES

(1) Léger, C.; Bertrand, P. Direct Electrochemistry of Redox Enzymes as a Tool for Mechanistic Studies. *Chem. Rev.* **2008**, *108*, 2379−2438.

(2) Armstrong, F. A.; Belsey, N. A.; Cracknell, J. A.; Goldet, G.; Parkin, A.; Reisner, E.; Vincent, K. A.; Wait, A. F. Dynamic Electrochemical Investigations of Hydrogen Oxidation and Production by Enzymes and Implications for Future Technology. *Chem. Soc. Rev.* **2009**, *38*, 36−51.

(3) Kaim, W.; Fiedler, J. Spectroelectrochemistry: the best of two worlds. *Chem. Soc. Rev.* **2009**, *38*, 3373−3382.

(4) Healy, A. J.; Reeve, H. A.; Vincent, K. A. Development of an Infrared Spectroscopic Approach for Studying Metalloenzyme Active Site Chemistry under Direct Electrochemical Control. *Faraday Discuss.* **2010**, *148*, 1−13.

(5) Dai, Y.; Zheng, Y.; Swain, G. M.; Proshlyakov, D. A. Equilibrium and Kinetic Behavior of $Fe(CN)_6^{3-/4-}$ And Cytochrome *c* in Direct Electrochemistry using a Film Electrode Thin-Layer Transmission Cell. *Anal. Chem.* **2011**, *83*, 542−548.

(6) Lu, H.; Rusling, J. F.; Hu, N. Protecting Peroxidase Activity of Multilayer Enzyme-Polyion Films Using Outer Catalase Layers. *J. Phys. Chem. B* **2007**, *111* (51), 14378−14386.

(7) Grochol, J.; Dronov, R.; Lisdat, F.; Hildebrandt, P.; Murgida, D. H. Electron Transfer in SAM/Cytochrome/Polyelectrolyte Hybrid Systems on Electrodes: A Time-Resolved Surface-Enhanced Resonance Raman Study. *Langmuir* **2007**, *23* (22), 11289−11294.

(8) Shi, G.; Sun, Z.; Liu, M.; Zhang, L.; Liu, Y.; Qu, Y.; Jin, L. Electrochemistry and Electrocatalytic Properties of Hemoglobin in Layer-by-Layer Films of SiO_2 with Vapor-Surface Sol-Gel Deposition. *Anal. Chem.* **2007**, *79* (10), 3581−3588.

(9) Davis, K. L.; Drews, B. J.; Yue, H.; Waldeck, D. H.; Knorr, K.; Clark, R. A. Electron-Transfer Kinetics of Covalently Attached

Cytochrome *c*/SAM/Au Electrode Assemblies. *J. Phys. Chem. C* **2008**, *112*, 6571−6576.
(10) Frasconi, M.; Mazzei, F.; Ferri, T. Protein Immobilization at Gold-Thiol Surfaces and Potential for Biosensing. *Anal. Bioanal. Chem.* **2010**, *398*, 1545−1564.
(11) Bowden, E. F.; Hawkridge, F. M.; Blount, H. N. Interfacial Electrochemistry of Cytochrome *c* at Tin Oxide, Indium Oxide, Gold, and Platinum-Electrodes. *J. Electoanal. Chem.* **1984**, *161*, 355−376.
(12) El Kasmi, A.; Leopold, M. C.; Galligan, R.; Robertson, R. T.; Saavedra, S. S.; El Kacemi, K.; Bowden, E. F. Adsorptive immobilization of cytochrome *c* on indium/tin oxide (ITO): electrochemical evidence for electron transfer-induced conformation changes. *Electrochem. Commun.* **2002**, *4*, 177−181.
(13) Topoglidis, E.; Palomares, E.; Astuti, Y.; Green, A.; Campbell, C. J.; Durrant, J. R. Immobilization and Electrochemistry of Negatively Charged Proteins on Modified Nanocrystalline Metal Oxide Electrodes. *Electroanalysis* **2005**, *17* (12), 1035−1041.
(14) Frasca, S.; von Graberg, T.; Feng, J.-J.; Thomas, A.; Smarsly, B. M.; Weidinger, I. M.; Scheller, F. W.; Hildebrandt, P.; Wollenberger, U. Mesoporous Indium Tin Oxide as a Novel Platform for Bioelectronics. *ChemCatChem* **2010**, *2*, 839−845.
(15) Hildebrandt, P.; Stockburger, M. Surface-Enhanced Resonance Raman Spectroscopy of Rhodamine 6G Adsorbed on Colloidal Silver. *J. Phys. Chem.* **1984**, *88*, 5935−5944.
(16) Geddes, C. D.; Parfenox, A.; Roll, D.; Fang, J.; Lankowicz, J. R. Electrochemical and Laser Deposition of Silver for use in Metal-Enhanced Fluorescence. *Langmuir* **2003**, *19*, 6236−6241.
(17) Hall, W. P.; Modica, J.; Anker, J.; Lin, Y.; Mrksich, M.; Van Duyne, R. P. A Conformation- and Ion-Sensitive Plasmonic Biosensor. *Nano Lett.* **2011**, *11*, 1098−1105.
(18) Casadio, F.; Leona, M.; Lombardi, J. R.; Van Duyne, R. P. Identification of Organic Colorants in Fibers, Paints, and Glazes by Surface Enhanced Raman Spectroscopy. *Acc. Chem. Res.* **2010**, *43* (6), 782−791.
(19) Glass, A. M.; Liao, P. F.; Bergman, J. G.; Olson, D. H. Interaction of Metal Particles with Adsorbed Dye Molecules: Absorption and Luminescence. *Opt. Lett.* **1980**, *5* (9), 368−370.
(20) Haes, A. J.; Zou, S.; Zhao, J.; Schatz, G. C.; Van Duyne, R. P. Localized Surface Plasmon Resonance Spectroscopy Near Molecular Resonances. *J. Am. Chem. Soc.* **2006**, *128*, 10905−10914.
(21) Gordon, R.; Sinton, D.; Kavanagh, K. L.; Brolo, A. G. A new generation of Sensors Based on Extraordinary Optical Transmission. *Acc. Chem. Res.* **2008**, *41* (8), 1049−1057.
(22) Boussaad, S.; Pean, J.; Tao, N. J. High-Resolution Multi-wavelength Surface Plasmon Resonance Spectroscopy for Probing Conformational and Electronic Changes in Redox Proteins. *Anal. Chem.* **2000**, *72*, 222−226.
(23) Lee, J. H.; Cha, J. N. Amplified Protein Detection through Visible Plasmon Shifts in Gold Nanocrystal Solutions from Bacteriophage Platforms. *Anal. Chem.* **2001**, *83* (9), 3516−3519.
(24) Liu, G. L.; Long, Y.-T.; Choi, Y.; Kang, T.; Lee, L. P. Quantized Plasmon Quenching Dips Nanospectroscopy via Plasmon Resonance Energy Transfer. *Nat. Methods* **2007**, *4* (12), 1015−1017.
(25) Zhao, J.; Das, A.; Schatz, G. C.; Sligar, S. G.; Van Duyne, R. P. Resonance Localized Surface Plasmon Spectroscopy: Sensing Substrate and Inhibitor Binding to Cytochrome P450. *J. Phys. Chem. C* **2008**, *112*, 13084−13088.
(26) Kalyuzhny, G.; Schneeweiss, M. A.; Shanzer, A.; Vaskevich, A.; Rubinstein, I. Differential Plasmon Spectroscopy as a tool for Monitoring Molecular Binding to Ultrathin Gold Films. *J. Am. Chem. Soc.* **2001**, *123*, 3177−3178.
(27) DiMilla, P. A.; Folkers, J. P.; Biebuyck, H. A.; Harter, R.; Lopez, G. P.; Whitesides, G. M. Wetting and Protein Adsorption of Self-Assembled Monolayers of Alkanethiolates Supported on Transparent Films of Gold. *J. Am. Chem. Soc.* **1994**, *116*, 2225−2226.
(28) Wanunu, M.; Vaskevich, A.; Rubinstein, I. Widely-Applicable Gold Substrate for the Study of Ultrathin Overlayers. *J. Am. Chem. Soc.* **2004**, *126*, 5569−5576.
(29) Hutter, E.; Pileni, M.-P. Detection of DNA Hybridization by Gold Nanoparticle Enhanced Transmission Surface Plasmon Resonance Spectroscopy. *J. Phys. Chem. B* **2003**, *107* (27), 6497−6499.
(30) Brolo, A. G.; Gordon, R.; Leathem, B.; Kavanagh, K. L. Surface Plasmon Sensor Based on the Enhanced Light Transmission through Arrays of Nanoholes in Gold Films. *Langmuir* **2004**, *20*, 4813−4815.
(31) Obare, S. O.; Ito, T.; Meyer, G. J. Controlling Reduction Potentials of Semiconductor-Supported Molecular Catalysts for Environment of Remediation of Organohalide Pollutants. *Environ. Sci. Technol.* **2005**, *39*, 6266−6272.
(32) van de Kamp, M.; Silvestrini, M. C.; Brunori, M.; van Beeumen, J.; Hali, F. C.; Canters, G. W. Involvement of the Hydrophobic Patch of Azurin in the Electron-Transfer Reactions with Cytochrome c_{551} and Nitrite Reductase. *Eur. J. Biochem.* **1990**, *194*, 109−118.
(33) Manetto, G. D.; Grasso, D. M.; Milardi, D.; Pappalardo, M.; Guzzi, R.; Sportelli, L.; Verbeet, M. P.; anters, G. W.; La Rosa, C. The Role Played by the α-Helix in the Unfolding Pathway and Stability of Azurin: Switching Between Hierarchic and Nonhierarchic Folding. *ChemBioChem* **2007**, *8*, 1941−1949.
(34) Brautigan, D. L.; Ferguson-Miller, S.; Margoliash, E. Mitochondrial Cytochrome *c*: Preparation and Activity of Native and Chemically Modified Cytochromes *c*. *Methods Enzymol.* **1978**, *53*, 128−164.
(35) Margoliash, E.; Frohwirt, N. Spectrum of Horse Heart Cytochrome *c*. *Biochem. J.* **1959**, *71*, 570−572.
(36) Jeuken, L. J. C. http://www.mnp.leeds.ac.uk/ljcjeuken/Jellyfit.htm.
(37) Jeuken, L. J. C.; Armstrong, F. A. Electrochemical Origin of Hysteresis in the Electron-Transfer Reactions of Adsorbed Proteins: Contrasting Behavior of the "Blue" Copper Protein, Azurin, Adsorbed on Pyrolytic Graphite and Modified Gold Electrodes. *J. Phys. Chem. B* **2001**, *105*, 5271−5282.
(38) Hinnen, C.; Parson, R.; Niki, K. J. Electrochemical and Spectroreflectance Studies of the Adsorbed Horse Heart Cytochrome *c* and Cytochrome c_3 from *D. Vulgaris*, Miyazaki Strain, at Gold Electrode. *J. Electroanal. Chem* **1983**, *147*, 329−337.
(39) Chen, X.; Ferrigno, R.; Yang, J.; Whitesides, G. M. Redox Properties of Cytochrome *c* Adsorbed on Self-Assembled Monolayers: A Probe for Protein Conformation and Orientation. *Langmuir* **2002**, *18*, 7009−7015.
(40) Collinson, M.; Bowden, E. F.; Tarlov, M. J. Voltammetry of Covalently Immobilized Cytochrome *c* on Self-Assembled Monolayer Electrodes. *Langmuir* **1992**, *8*, 1247−1250.
(41) Nakano, K.; Yoshitake, T.; Yamashita, Y.; Bowden, E. F. Cytochrome *c* Self-Assembly on Alkanethiol Monolayer Electrodes as Characterized by AFM, IR, QCM, and Direct Electrochemistry. *Langmuir* **2007**, *23*, 6270−6275.
(42) Gomez-Mingot, M.; Iniesta, J.; Montiel, V.; Kadara, R. O.; Banks, C. E. Screen Printed Graphite Macroelectrodes for the Direct Electron Transfer of Cytochrome. *c*. *Analyst* **2011**, *136*, 2146−2150.
(43) Leopold, M. C.; Bowden, E. F. Influence of Gold Substrate Topography on the Voltammetry of Cytochrome c Adsorbed on Carboxylic Acid Terminated Self-Assembled Monolayers. *Langmuir* **2002**, *18* (6), 2239−2245.
(44) Bard, A. J.; Faulkner, L. R. *Electrochemical Methods: Fundamentals and Applications*, 2nd ed.; John Wiley & Sons, Inc.: New York, 2001.
(45) Laviron, E. Voltammetry of Adsorbed Molecules. In *Electroanalytical Chemistry*; Bard, A. J., Ed.; Marcel Dekker: New York, 1982; Vol. *12*, pp 53−157.
(46) Takano, T.; Kallai, O. B.; Swanson, R.; Dickerso., R. E. Structure of Ferrocytochrome *c* at 2.45 Å Resolution. *J. Biol. Chem.* **1973**, *248* (15), 5234−5255.
(47) Fleming, B. D.; Praporski, S.; Bond, A. M.; Martin, L. L. Electrochemical Quartz Crystal Microbalance Study of Azurin Adsorption onto an Alkanethiol Self-Assembled Monolayer on Gold. *Langmuir* **2008**, *24*, 323−327.
(48) Bramblett, A. L.; Boeckl, M. S.; Hauch, K. D.; Ratner, B. D.; Sasaki, T.; Rogers, J. W. Jr. Determination of Surface Coverage for

Tetraphenylporphyrin Monolayers using Ultraviolet Visible Absorption and X-Ray Photoelectron Spectroscopies. *Surf. Interface Anal.* **2002**, *33*, 506−515.
(49) Chi, Q. J.; Zhang, J. D.; Nielsen, J. U.; Friis, E. P.; Chorkendorff, I.; Canters, G. W.; Anderson, J. E. T.; Ulstrup, J. Molecular Monolayers and Interfacial Electron Transfer of *Pseudomonas Aeruginosa* Azurin on Au(111). *J. Am. Chem. Soc.* **2000**, *122*, 4047−4055.
(50) Fristrup, P.; Grubb, M.; Zhang, J.; Christensen, H. E. M.; Hansen, A. M.; Ulstrup, J. Voltammetry of Native and Recombinant Pseudomonas Aeruginosa Azurin on Polycrystalline Au- and Single-Crystal Au(111)-Surfaces Modified by Decanethiol Monolayers. *J. Electoanal. Chem.* **2001**, *511*, 128−133.
(51) Zhang, J.; Chi, Q.; Nielsen, J. U.; Hansen, A. M.; Anderson, J. E. T.; Wackerbarth, H.; Ulstrup, J. Organized Monolayers of Biological Macromolecules on Au(111) Surfaces. *Russ. J. Electrochem.* **2002**, *38*, 68−76.
(52) Andolfi, L.; Bruce, D.; Cannistraro, S.; Canters, G. W.; Davis, J. J.; Hill, H. A. O.; Crozier, J.; Verbeet, M. P.; Wrathmell, C. L.; Astier, Y. The Electrochemical Characteristics of Blue Copper Protein Monolayers on Gold. *J. Electroanal. Chem.* **2004**, *565*, 21−28.
(53) Shleev, S.; Tkac, J.; Christenson, A.; Ruzgas, T.; Yarapolov, A. I.; Whittaker, J. W.; Gorton, L. Direct Electron Transfer between Copper-Containing Proteins and Electrodes. *Biosens. Bioelectron.* **2005**, *20*, 2517−2554.
(54) Vargo, M. L.; Gulka, C. P.; Gerig, J. K.; Manieri, C. M.; Dattelbaum, J. D.; Marks, C. B.; Lawrence, N. T.; Trawick, M. L.; Leopold, M. C. Distance Dependence of Electron Transfer Kinetics for Azurin Protein Adsorbed to Monolayer Protected Nanoparticle Film Assemblies. *Langmuir* **2009**, *26*, 560−569.
(55) Ressine, A.; Vaz-Dominguez, C.; Fernandez, V. M.; De Lacey, A. L.; Laurell, T.; Ruzgas, T.; Shleev, S. Bioelectrochemical Studies of Azurin and Laccase confined in Three-Dimensional Chips Based on Gold-Modified Nano-/Microstructured Silicon. *Biosens. Bioelectron.* **2010**, *25* (5), 1001−1007.
(56) Davis, J. J.; Burgess, H.; Zauner, G.; Kuznetsova, S.; Salverda, J.; Aartsma, T. Canters, G. W., Monitoring Interfacial Bioelectrochemistry using a FRET Switch. *J. Phys. Chem. B* **2006**, *110*, 20649−20654.
(57) Chi, Q.; Zhang, J.; Anderson, J. E. T.; Ulstrup, J. Ordered Assembly and Controlled Electron Transfer of the Blue Copper Protein Azurin at Gold (111) Single-Crystal Substrates. *J. Phys. Chem. B* **2001**, *105*, 4669−4679.
(58) Guo, Y.; Zhao, J. W.; Yin, Z. G., X. L.; Tian, Y. N. Electrochemistry Investigation on Protein Protection by Alkanethiol Self-Assembled Monolayers against Urea Impact. *J. Phys. Chem. C* **2008**, *112*, 6013−6021.
(59) Williams, P. M.; Shakesheff, K. M.; Davies, M. C.; Jackson, D. E.; Roberts, C. J.; Tendler, S. J. B. Blind Reconstruction of Scanning Probe Image Data. *J. Vac. Sci. Technol. B* **1996**, *14*, 1557−1562.
(60) Villarrubia, J. S. Algorithms for scanned probe microscope image simulation, surface reconstruction, and tip estimation. *J. Res. Natl. Inst. Stand. Technol.* **1997**, *102*, 425−454.